HHS Public Access

Author manuscript

Nat Med. Author manuscript; available in PMC 2017 January 04.

Published in final edited form as:

Nat Med. 2016 August ; 22(8): 889–896. doi:10.1038/nm.4116.

Targeting β1-Integrin Signaling Enhances Regeneration in Aged and Dystrophic Muscle in Mice

Michelle Rozo[1,2,+], **Liangji Li**[1,2,+], and **Chen-Ming Fan**[1,2,*]

[1]Department of Biology, Johns Hopkins University, Baltimore, Maryland, USA

[2]Department of Embryology, Carnegie Institution of Washington, Baltimore, Maryland, USA

Abstract

Interactions between stem cells and their microenvironment, or niche, are essential for stem cell maintenance and function. Our knowledge of the niche for the skeletal muscle stem cell, i.e. the satellite cell (SC), is incomplete. Here we show that β1-integrin is an essential niche molecule that maintains SC homeostasis, and sustains the expansion and self-renewal of this stem cell pool during regeneration. We further show that β1-integrin cooperates with FGF-2, a potent growth factor for SCs, to synergistically activate their common downstream effectors Erk and Akt. Importantly, SCs in aged mice display altered β1-integrin activity and insensitivity to FGF-2. Augmenting β1-integrin activity with a monoclonal antibody restores FGF-2 sensitivity and improves regeneration after experimentally-induced muscle injury. The same treatment also enhances regeneration and function of dystrophic muscles in *mdx* mice. Therefore, β1-integrin senses the SC niche to maintain responsiveness to FGF-2, and this integrin represents a potential therapeutic target for pathological conditions of the muscle in which the stem cell niche is compromised.

Sarcopenia, the slow progressive loss of skeletal muscle mass concomitant with advancing age, affects elderly people. Age-related muscle wasting is characterized by loss of muscle quantity and quality due to changes in muscle metabolism, function and regeneration[1]. The poor regeneration of aged muscle is not attributed solely to the loss of stem cells (i.e. satellite cells, SCs)[2,3], although SC numbers decline during aging in mice and humans. Instead, the impaired regeneration is linked to aged-related changes in both extrinsic systemic and local environments as well as intrinsic defects[4–11].

*Author of correspondence: Chen-Ming Fan; tel: 410-246-3022; fan@ciwemb.edu.
+These two authors contribute equally.

The authors declare no conflict of interest.

Accession codes

All sequencing data can be found at NCBI Sequence Read Archive (SRA), SRP# Study accession: SRP070128.

Author Contributions

M.R. and C.-M.F. conceptualized the study. M.R. performed experimental analysis of the mouse mutant, FACS and RNA-seq data, and demonstrated the utility of TS2/16. L.L. performed mechanistic experiments to investigate integrin-FGF synergy, and conducted *in situ* muscle force measurement. C.-M.F. initiated and supervised the project. All three authors wrote, discussed and edited the manuscript.

Competing financial interests

The authors declare no competing financial interests.

A well-studied niche signal, fibroblast growth factor-2 (FGF-2), has important roles in driving SC proliferation. SCs are maintained in a quiescent state by repressing FGF-2 signals[7]. Aging increases the level of FGF-2 in skeletal muscle and decreases the level of FGF signaling inhibitor Spry1 in SCs, which results in loss of a portion of the SC pool due to breaking quiescence[2]. Paradoxically, aged SCs are non-responsive to FGF-2 during their proliferation and self-renewal[9]. Inhibiting FGF signaling in aged SCs rescues the quiescent phenotype at the expense of regeneration[2], whereas ectopically activating FGF receptor 1 (FGFR1) rescues the proliferative capacity of aged SCs[9]. It is unclear what underlies the differential requirement for FGF and what causes the desensitization of FGFR1, but changes in interactions with other cell surface proteins may contribute.

Integrins adhere to the extra cellular matrix (ECM) to cooperate with different growth factor signaling pathways depending on the cell type and context[12,13]. Integrins are heterodimers comprised of an α and a β chain that function to link the ECM to the actin cytoskeleton[14]. There are 18 α and eight β chains, which can form at least 28 isoforms. Of particular relevance to skeletal muscles are α7 and β5 integrins and laminin α2 as their mutations cause muscular dystrophies[14, 15]. Inactivation of *Itgb1* (encoding β1-integrin) in the embryonic muscle lineage causes defects in muscle cell migration, fusion, and sarcomere assembly, but not progenitor proliferation[16]. Although β1-integrin is conspicuously expressed by adult SCs, its role has not been examined, especially with respect to modulating FGF signaling. Here we show that β1-integrin is the sensor of the SC niche that maintains quiescence of SCs during homeostasis and it also cooperates with FGF signaling to promote SC proliferation and renewal after injury. We further demonstrate that activating β1-integrin signaling restores FGF sensitivity in aged SCs and improves muscle regeneration. Activating β1-integrin in the *mdx* mouse[17], a model for Duchenne muscular dystrophy, can also promote SC expansion and improve function. We propose that β1-integrin is a potential therapeutic target of pathological conditions in which the SC niche is compromised.

RESULTS

SCs without β1-integrin cannot maintain quiescence

To define the function of β1-integrin in adult SCs, we employed a $Pax7^{\text{Cre-ERT2(CE)}}$ driver[18] for tamoxifen (tmx) inducible gene inactivation of a *Itgb1* conditional allele ($Itgb1^{f}$;[19]) in SCs. Cre reporter alleles $R26R^{\text{YFP}}$ or $R26R^{\text{LacZ}}$ were included for lineage marking and assessing recombination efficiency (Supplementary Fig. 1a–c;[18]). Three days (3 d) after tmx regimen, YFP^{+} conditional mutant ($Itgb1^{-/-}$) SCs no longer had detectable β1-integrin (Supplementary Fig. 1d,e) but maintained Pax7 expression, compared to control SCs (Fig. 1a). To assess whether β1-integrin loss affected SC niche occupancy, we followed lineage-marked cells up to 180 d (Fig. 1b–d). The number of $Itgb1^{-/-}$ SCs was unchanged compared to that of controls 7 d after tmx regimen, but reduced to about half of that in controls at 21 d. $Itgb1^{-/-}$ SCs continued to decline over time, but were not completely lost by 180 d. We did not detect programmed cell death (PCD) of $Itgb1^{-/-}$ SCs at these time points (Supplementary Fig. 1f). Instead, lineage-labeled myofibers suggest mutant SC loss via differentiation and incorporation into existing muscle fibers (Fig. 1b,c).

To test whether their slow loss was indeed due to spurious activation and differentiation, we performed continuous BrdU administration for 30 d. A significant portion of *Itgb1*$^{-/-}$ SCs incorporated BrdU during this period, revealing aberrant cell cycle entry (Fig. 1e). A greater fraction of MyoD^{+} cells was also detected in the mutant, compared to the control (Fig. 1f), supporting spurious differentiation. Given that there was no increase in SCs, those that became activated likely had limited proliferative capacity. Furthermore, polarity proteins m-cadherin and Par3 were not localized appropriately in *Itgb1*$^{-/-}$ SCs (Supplementary Fig. 2), suggesting mutant SC loss is associated with polarity defects. We conclude β1-integrin senses quiescent SC-niche to maintain polarity and prevent spurious activation and differentiation.

SCs without β1-integrin cannot sustain proliferation upon injury

To assess whether *Itgb1*$^{-/-}$ SCs could support regeneration, we conducted muscle injury by cardiotoxin at 3 d post tmx (Supplementary Fig. 3a). We performed these and all subsequent assays when mutant SC number was normal in order to appropriately analyze the separate role of β1-integrin in SC-driven muscle regeneration. Severely defective regeneration was observed at 5, 10, and 30 d post-injury (Fig. 1g–i; Supplementary Fig. 3b–d). Consistent with embryonic studies[16], adult *Itgb1*$^{-/-}$ myoblasts migrated and fused poorly *in vitro* (Supplementary Fig. 3e–g), which explains the reduced diameter of regenerated fibers (Fig. 1i).

The drastic reduction in regenerated fiber numbers (Fig. 1h) in the mutant suggests a SC expansion defect. To test this, we pulsed proliferative cells with EdU from 2 to 5 d daily after injury. *Itgb1*$^{-/-}$ SCs proliferated normally at d 2, but did not sustain the same proliferative rates in ensuing days as control SCs (Fig. 2a,b). Although PCD did not appear to be a contributor to reduced mutant cells (Supplementary Fig. 1f), we cannot exclude other cell elimination processes. To ascertain the molecular changes in *Itgb1*$^{-/-}$ SCs, we performed cell cycle analyses of FACS-isolated YFP^{+} control and mutant SCs[20] in culture (Fig. 2c–f). Compared to control cells, mutant cells had lower levels of cyclins D1 and D2, and misregulated cell cycle showing an increased fraction of G1 and a decreased faction in S phase at 72 h. Gene expression profiles of control and mutant SCs showed no differences up to 24 h in culture, but became progressively different at 48 and 72 h (Supplementary Fig. 4). At 72 h, many genes associated with muscle differentiation were up-regulated in mutant cells (Fig. 2g). These data are consistent with the role of β1-integrin in sustaining cyclin D levels and G1/S transition in other cell types[13, 21].

To determine whether there was a defect in SC self-renewal, we monitored Pax7^{+} cells in the regenerative area of *Itgb1*$^{-/-}$ mice. Pax7^{+} cell numbers were significantly reduced at d 3 and d 4, and not present after d 5 (Fig. 3a,b). Although there were fewer MyoD^{+} mutant cells, ratios of MyoD^{+} to Pax7^{+} mutant cells were higher than those of control cells (Supplementary Fig. 5a,b), indicating that *Itgb1*$^{-/-}$SCs turned off Pax7 and failed to self-renew. Thus, β1-integrin is required for SC proliferation and self-renewal to drive muscle regeneration.

β1-integrin crosstalks with FGF signaling in SCs

Activation of integrins by the ECM cooperates with receptor tyrosine kinases (RTKs), including FGFR, to activate Erk MAP kinases and drive proliferation in many cell types[12,13,21–24]. FGF-2 stimulates myoblast proliferation via the same effectors[25], which may involve integrin signaling. We therefore examined whether *Itgb1*$^{-/-}$ myoblasts were defective in FGF-2 responsiveness with or without fibronectin, an ECM molecule originally used to demonstrate integrin-RTK crosstalk[21,24]. The phosphorylation levels of their common downstream effectors, Erk and Akt (pErk1, pErk2 and pAkt) were assessed (Fig. 3c,d). Control cells responded better to FGF-2 in the presence of fibronectin; low levels of FGF-2 was sufficient to phosphorylate Erk and, to a lesser extent Akt. In contrast, fibronectin or high levels of FGF-2 alone only weakly activated Erk and Akt. Mutant cells were indeed defective in responding to FGF-2 in the presence of fibronectin. Importantly, high levels of FGF-2 could partially restore cooperativity, likely due to compensation by other fibronectin-binding integrins in *Itgb1*$^{-/-}$ cells.

We next assessed the relevance of the cooperativity between integrin and FGF signaling in the SC. Using the single myofiber assay[9] to examine SC fates, we determined that the majority of control SCs maintained Pax7 expression (Pax7^{+}MyoD^{-} and Pax7^{+}MyoD^{+}). Addition of FGF increased the Pax7^{+}MyoD^{+} expanding population but did not alter the Pax7^{+}MyoD^{-} self-renewed fraction (Fig. 3e,f). In contrast, the majority of mutant SCs were committed to differentiate, expressing only MyoD, at the expense of Pax7^{+}MyoD^{+} and Pax7^{+}MyoD^{-} fractions. The latter two populations were partially rescued by FGF-2 addition, again suggesting compensation by other integrins. As SCs express almost all integrin subtypes[26], we tested whether the RGD peptide, a broad-spectrum integrin-binding competitor that interferes with ECM engagement[14], was sufficient to disrupt FGF response. SCs treated with RGD peptide had a reduced fraction of Pax7^{+}MyoD^{+}cells, which could not be rescued by FGF-2 (Supplementary Fig. 5c–e). Thus, RGD-binding integrins in the SC, including those containing β1-integrin, cooperate with FGF-2. SC self-renewal has been associated with FGF stimulation of asymmetric p38α/βMAPK phosphorylation[9,27]. Fewer *Itgb1*$^{-/-}$ SCs displayed polarized pp38, relative to controls, and FGF-2 could increase the fraction of mutant SCs with polarized pp38 (Fig. 3g,h). Together, we have uncovered a mechanism for β1-integrin in sustaining SC expansion and self-renewal.

Aged SCs are defective in integrin activity

The characteristics of *Itgb1*$^{-/-}$ SCs are similar to aged SCs; both are gradually lost from the niche[2], cannot sustain proliferation[28], are committed to differentiation[5], and are defective in self-renewal[9]. Given that ECM composition[29] and stiffness[30] change in aged muscles, we wondered whether the aged environment impacts β1-integrin or overall integrin activity, thereby desensitizing aged SCs to FGF-2[9]. To probe for changes in integrin activity in aged SCs, we first used an antibody (9EG7) that recognizes the “high-affinity” ligand-bound active β1-integrin[31,32] on young and aged SCs. The majority of young myofiber-associated SCs displayed well-aligned basal membrane-bound β1-integrin in its active conformation, mirroring total β1-integrin (compare Fig. 4a to Fig. 1a). Despite a basally localized pattern of total β1-integrin (Supplementary Fig. 6a), more aged SCs displayed active β1-integrin in abnormal patterns: in disorganized puncta or undetectable (Fig. 4a,b). To ascertain age-

associated changes in overall integrin activity, we monitored spatial patterns of their common effectors: integrin-linked kinase (ILK), parvin, and paxillin (Fig. 4c). ILK, parvin and paxillin were localized to the laminar side in young SCs as expected. In contrast, aged SCs showed disorganized distribution patterns of these effectors. Vinculin, which binds to actin but not directly to integrin[33], encircled young SCs and this pattern was slightly disorganized in aged SCs. Thus, aged SCs display abnormal localization and disparate changes of common integrin effectors, reflecting a dysregulation of overall integrin activity.

If dysregulated integrin signaling underlies the dysfunction of aged SCs, activating β1-integrin alone may be sufficient for rescue. To test this, we injected injured muscles with a β1-integrin-activating antibody TS2/16 (Ref. 34) (Fig. 4d–f). Robust muscle regeneration was observed in control young mice injected with vehicle (YV). The RGD peptide repressed muscle regeneration in young mice (YI). While TS2/16 did not enhance the already robust regeneration in young animals (YA), it improved regeneration in aged mice (AA) to a level comparable to the young. As controls, we showed that TS2/16 did not rescue regeneration of *Itgb1*$^{-/-}$ muscle, but could activate β1-integrin-dependent signaling (Supplementary Fig. 7a–d). Thirty days later, regenerated muscles still had measurable improvement by a single dose of TS2/16 (Supplementary Fig. 7e–g).

To determine whether TS2/16 improves SC function, we applied it to myofiber-associated aged SCs and assessed their expansion and Pax7 expression. Neither the IgG control, nor TS2/16 or FGF-2 treatment alone showed an effect. TS2/16 and FGF-2 together increased the fraction of Pax7^{+} cells, the number of fiber-associated myogenic cells, and the fraction of SCs displaying polarized pp38 (Fig. 5a–c and Supplementary Fig. 8). Since TS2/16 alone is sufficient *in vivo,* we surmise that muscle damage releases a sufficient amount of FGF-2 to cooperate with TS2/16-activated β1-integrin in aged SCs. Mechanistically, we found that TS2/16 increased the fraction of aged SCs on myofibers with detectable FGFR1, relative to control IgG (Fig. 5d,e). Although not sufficient to enhance expansion, TS2/16 alone increased the proportion of aged SCs with detectable phosphorylated FGFR (pFGFR). TS2/16 and FGF-2 together stimulated pFGFR in almost all aged SCs (Fig. 5f,g), consistent with their dual requirement for enhancing aged SC expansion. Associations between FGFR and α-integrin[35] or αvβ3-integrin[36] were suggested to underlie FGF-integrin cooperativity. We show here that FGFR1 can associate with β1-integrin, and that TS2/16 enhances their association (Fig. 5h). These data indicate that TS2/16 operates at multiple layers to enhance FGF signaling and restore the responsiveness in aged SCs.

Activating β1-integrin improves dystrophic muscles

The positive effect of TS2/16 on regeneration in aged environment led us consider whether it might be beneficial in another context of impaired muscle regeneration: muscular dystrophy. For this, we employed the *mdx* mouse model, which lacks dystrophin expression due to a nonsense mutation[17]. As the *mdx* muscle contains disorganized ECM, we anticipated more Pax7^{+} SCs residing outside of the myofiber lamina, relative to those in the control (C57BL/10; Supplementary Fig. 9a–c). Additionally, *mdx* SCs associated with myofibers displayed abnormal patterns of active β1-integrin (Supplementary Fig. 6b,c). We administered TS2/16 into the TA muscle of *mdx* mice and found that a single dose was

sufficient to promote the expansion of myogenic cells, as shown by increased EdU incorporation 3 d after treatment (Fig. 6a,b). We extended TS2/16 treatment to 4 weekly injections (Fig. 6c) and found cross-sectional area and muscle fiber diameter were increased, relative to those treated with control IgG (Fig. 6c–e). The percentage of $Pax7^+$ cells outside of myofiber lamina also was reduced, reflecting an improvement in SC-niche interaction (Supplementary Fig. 9c–e). As α7β1-integrin binds to laminin, the ECM component that engages with the dystrophin complex, activating β1-integrin likely also enhances muscle fiber integrity in *mdx* mice via improved connection to the ECM.

To determine whether the above long-term regimen resulted in functional rescue, we compared the contractile properties of IgG- and TS2/16-treated *mdx* TA muscles *in situ*; wt and untreated *mdx* TA muscles were done in parallel for references (Fig. 6f–j). TS2/16-treated *mdx* muscles had reduced cross sectional areas than those of *mdx* and IgG-treated *mdx* muscles, consistent with a reversal from hypertrophic pathology. Significantly, TS2/16-treated muscles showed strength improvements in a variety of measurements, including single twitch force, maximum isometric tetanic force, force-frequency relationship, time to fatigue, and fatigue index. Activating β1-integrin may therefore be a viable therapeutic means to improve muscle repair and function in diseased conditions.

DISCUSSION

Our results frame a model in which β1-integrin acts as a sensor of the SC niche that declines in function upon aging (Supplementary Fig. 10). Because $Itgb1^{-/-}$ cells show compromised pErk induction by FGF-2, their quiescence breaking is more likely due to cell polarity defects than overt FGF-Erk signaling[2]. In the regenerative context, β1-integrin has a distinct role in cooperating with FGF-2 to drive SC proliferation and renewal. In aged muscle, changes in ECM[29,30] impose physiological relevant alterations in integrin activity (see accompanying paper, Lukjanenko et al.), which likely contribute to the decline of SC's FGF sensitivity. The current view regarding FGF and aging SCs is puzzling. Aging SCs are sensitive to increased FGF-Erk signaling, causing quiescence break and loss[2], and yet aged SCs are insensitive to FGF-2 for expansion *in vitro*[9]. Our study provides a potential explanation: A fraction of aging SCs with sufficient integrin activity cooperates with increasing FGF-2 to break quiescence and becomes lost, while those with dysregulated integrin activity insufficient to support FGF signaling, remain. As such the remaining aged SCs cannot support robust regeneration after injury, unless integrin activity is re-established, e.g. by TS2/16, to restore FGF signaling.

While activating β1-integrin alone can improve regeneration in both aged and dystrophic muscles, it may prove more effective to target all integrins relevant to SC expansion and FGF-sensitivity, e.g. RGD-binding integrins. There are minimally eight integrins (three of which contain β1-integrin) that bind to the RGD motif, which is the integrin binding site of many ECM molecules, including fibronectin[14]. While β1-integrin and fibronectin cooperate with FGF-2, we cannot exclude contributions by other RGD-containing ECM components. Conversely, as SCs express almost all α- and β-integrins[26], defining the contribution of each integrin in this context may take considerable efforts. Despite the complexity, our findings help to explain why ECM implantation can enhance muscle regeneration[37]. Future

investigation into how the integrin-FGF axis intersects with other pathways, e.g. Stat3, to regulate SC function, is important. Although *Stat3* expression is not changed in *Itgb1*$^{-/-}$ SCs, *Stat3* is up-regulated in activated SCs[38] and inhibiting Stat3 enhances regeneration in aging and dystrophic contexts[10,11]. It would be remiss if we do not mention that other than FGF-2, integrins can cooperative with many growth factors[12] that may also contribute to SC function. We provide here a proof of principle study that may be broadly applicable to muscle diseases involving SC niche dysfunction, but further refinement is needed for this method to become a viable treatment. Given the role of integrin in other stem cell populations[19,39], knowledge derived from our study likely have broader implications for aging and decline of function of stem cells in general.

Online Methods

Animal studies

Animal experiments in this study were performed in accordance with protocols approved by the Institutional Animal Care and Use Committee (IACUC) of the Carnegie Institution for Science (Permit number A3861-01). The *Pax7*$^{\text{cre-ERT2(CE)}}$ allele (B6;129-*Pax7*$^{\text{tm2.1(cre/ERT2)}}$*Fan*/J) has been described[18]. The *Itgb1*$^{\text{f}}$ allele (B6;129-Itgb1tm1Efu/J)[19] and the *R26R*$^{\text{lacZ}}$ (B6.129S4-*Gt*(*ROSA*)*26Sortm1Sor*/J)[40] and *R26R*$^{\text{YFP}}$ (B6.129X1-*Gt*(*ROSA*)*26Sor*$^{\text{tm1(EYFP)}}$*Cos*/J)[41] reporter mice were obtained from the Jackson Laboratory. The experimental mice used in this study were *Pax7*$^{\text{CE/+}}$; *Itgb1*$^{\text{f/f}}$; *R26R*$^{\text{LacZ/LacZ}}$, *Pax7*$^{\text{CE/+}}$; *Itgb1*$^{\text{f/f}}$; *R26R*$^{\text{YFP/YFP}}$, or *Pax7*$^{\text{CE/+}}$; *Itgb1*$^{\text{f/f}}$, referred to as *Itgb1*$^{-/-}$. Reporter alleles were chosen based on the assay: YFP is preferable for immunofluorescence, and necessary for live-imaging and FACS sorting, while LacZ is useful for histological analyses. Controls used were *Pax7*$^{\text{CE/+}}$; *R26R*$^{\text{LacZ/LacZ}}$, *Pax7*$^{\text{CE/+}}$; *R26R*$^{\text{YFP/YFP}}$, or *Pax7*$^{\text{CE}}$. For young versus aged comparisons, mice were used at 3 – 6 month of age (young) or 18 – 24 month of age (aged). For non-lineage marked SC studies, aged C56/BL6 mice were used (JAX and NIH). Sex was mixed. For dystrophic muscle studies, control and *mdx* male mice of C57BL/10 background (JAX) were used at 3 – 4 months of age.

Mice were given tamoxifen (tmx, 20 mg/ml in corn oil (Sigma)) at 3 mg per 40 g body weight per intraperitoneal injection, once a day consecutively for 5 days. All experiments except where noted were conducted 3 d after the final injection. For injury, mice were anesthetized using 2,2,2-Tribromoethanol (Sigma), which was dissolved in 2-methyl-2-butanol (Sigma) as 100% (w/v) stock solution, diluted 1:80 in PBS, and injected intraperitoneally at 10 μl per g body weight. For *Itgb1*$^{-/-}$ vs. control injury, 50 μl of 10 μM cardiotoxin (CTX; Sigma) was injected using an insulin syringe (U-100; Becton Dickinson) into TA muscles. Animals were then harvested at post injury time points stated in the text and legends. For short-term daily *in vivo* proliferation assay, EdU (Invitrogen) was given by intraperitoneal injection at 0.1 mg per 20 g bodyweight per injection, at 2, 3, 4, or 5 d after injury. Animals were harvested 24 h after injection. For long-term BrdU incorporation, mice were fed with 0.8 mg/ml of BrdU in drinking water for 1 month. For labeling Pax7^{+} cells, both aged and young *Pax7*$^{\text{CE}}$; *R26R*$^{\text{YFP/YFP}}$ animals were injected with tmx as described above and harvested for analysis or single fiber culture. For needle tract injury, TA muscles

were injured as described previously[6]. Two d post injury, TA muscles received 6 X 10 μl anti-TLR2 [TS2/16] (10 μg/ml), 60 μl vehicle control (mouse IgG, 10 μg/ml), RGD peptide (10 μg/ml), or scrambled peptide (10 μg/ml) by intramuscular injections. Muscles were harvested 3 d after these injections for analysis. For *mdx* mice, 10 μg (in 25 ul) of vehicle control IgG or TS2/16 were injected to each TA muscles, either by single injection or repeated 4 times weekly.

Antibodies and recombinant proteins

Antibodies against pan-β1-integrin, Cleaved Caspase-3, Parvin, pp38, pAkt, Akt, pErk1/2, Erk1/2, pFAK, FAK, pFGFR, and FGFR1 were from Cell Signaling (4706, 5A1E, 4026, 9216, 4060, 4691, 4370, 4695, 8556, 13009, 3471, and 9740, respectively). Anti-GAPDH antibody was from Chemicon (MAB374). Antibodies against activated β1-integrin and Paxillin were from BD Biosciences (9EG7 and 610619, respectively). For detecting β1-integrin by Western blot and Par3 in SCs on single fibers, MAB1997 and 07-330, respectively, from Millipore were used. Anti-TLR2 [TS2/16] and control mouse IgG were from Abcam (ab1119333 and ab37355, respectively). Anti-BrdU antibody was from Exalpha (A250P). GFP antibodies were from Invitrogen (G10362, rabbit) and Aves (GFP-1020, chick). Antibodies against eMyHC, MHC, and Pax7 were from Developmental Studies Hybridoma Bank (F1.652, MF20, and PAX7, respectively). Anti-PAX7 of rabbit origin (PA1-117; Thermo) was also used for co-staining with Abs of mouse origin. Anti-Laminin and anti-Vinculin were from Sigma (L9393 and V9131, respectively). Antibodies against Cyclin A, Cyclin B1, Cyclin D1, Cyclin D2, Cyclin D3, Cyclin E, ILK, and MyoD were from Santa Cruz Biotech (sc-596, sc-245, sc-717, sc-593, sc-182, sc-198, sc-20019, sc-81471, and sc-304, respectively). RGD and scrambled peptides were from Santa Cruz Biotech and AnaSpec. Carrier-free FGF-2 was purchased from R&D systems and dissolved and stored at −80 °C. The working dilution of the above antibodies and concentrations of recombinant proteins were typically used as recommended by the companies, unless otherwise specified below or in the text and legends in assay-dependent manners.

Muscle sample processing

TA muscles were harvested, fixed for 8 min in ice cold 4% paraformaldehyde (EMS) in phosphate buffered saline (PBS), incubated sequentially in 10% and 20% sucrose/PBS overnight, frozen in isopentane (Sigma)/liquid nitrogen, and stored at −80 °C freezer until cryosectioning. Cross-sections (10 μm) were stained with Haematoxylin and Eosin (H&E, Surgipath), Gomori's one-step trichrome staining kit (Polysciences), or subjected to X-gal (Sigma) reactions as described previously[42], or used for immunostaining and EdU reactions (see below).

SC isolation and myoblast culture

YFP-marked cells were isolated following a published protocol[17]. Briefly, for SC preparation, muscles were dissected and incubated in 0.2% Collagenase Type I (Sigma) in DMEM (Gibco) at 37 °C with gentle shaking for 1.5 h. Muscle was then triturated in 10% FBS in DMEM, washed with PBS, and incubated in 0.2% Dispase (Gibco) in DMEM at 37 °C with gentle shaking for 30 minutes. Cells were filtered through a 70 μm cell strainer (VWR) and subjected to cell sorting using the BD FACS ARIA III, gating first for cell size

using forward and side scatter, and then for YFP fluorescence. FACS Diva (for cell isolation) software was used. Cells were then used for downstream analyses. For cell cycle analysis, migration, and programmed cell death assays, as well as protein extracts for Western blotting (see below), or RNA isolation for RNA-seq (see below) over a time course, cells were cultured in 'minimal' growth media (10% Horse Serum (HS), 1% Pen/Strep, 1% Glutamax in DMEM with high glucose; GIBCO) on Matrigel (BD biosciences) coated tissue culture dishes. For differentiation and fusion, cells were cultured in media containing 2% HS on matrigel. For Erk and Akt signaling assays (see below), when considerably more cells were needed, cells were expanded as myoblast cultures in 'enriched' growth media (20% Fetal Bovine Serum, 5% Horse Serum, 1% Pen/Strep, 1% Glutamax (Gibco), 0.1% chick embryo extract (MP biomedicals), and 10 ng/ml FGF (R&D systems)) on Matrigel, until sufficient cell numbers were reached, typically in 5–7 days. All cell cultures were placed in 37 °C tissue culture incubators with 5% CO_2.

Myofibers with associated SCs were isolated from extensor digitorum longus (EDL) muscles by 1.5 h digestion in 0.2% Collagenase Type I in DMEM at 37 °C. The digested muscle was then transferred to tissue culture dishes containing DMEM, 1% Pen/Strep, and 1% Glutamax. Live myofibers were isolated with a fire polished glass pipette. Isolation of individual myofibers by pipette was repeated to remove dead myofibers and cellular debris. They were either immediately fixed for assay (e.g. probe for activated β1-integrin) or placed in DMEM, 10% Horse Serum, 1% Penn/Strep, and 1% Glutamax with daily medium and reagent changes. Please note that this minimal growth medium contains no additional additives. Pending on the assays, myofibers were cultured for different amount of time before fixation. For Par3, pp38, FGFR1, and pFGFR analysis, myofibers were cultured for 36 h. For self-renewal assays with Pax7 and MyoD expression, 48 - 96 h cultures were used (specified in text or figure legend). They were either cultured with or without FGF-2 (10 ng/ml), and with or without IgG or TS2/16 (10 μg/ml). Phosphatase Inhibitor Cocktail Set II (Calbiochem) was used as directed during fixation.

For FGF and fibronectin stimulation, we modified the condition described previously for other cell types[18,21]. The day of experiment, control and *Itgb1*$^{-/-}$ myoblasts were detached by 2mM EDTA in serum-free base-media (SFBM, high glucose DMEM, 0.5% BSA, Pen/Strep), washed twice and cultured in SFBM on petri-dish as suspension for 2 h to minimize residual effect of growth factors and contact-dependent signaling from prior culture condition. 50,000 cells were then transferred to each well of a 12-well dish containing SFBM with or without fibronectin (10 μg/ml) for 20 min. The wells were either coated with Sigma-cote (to prevent attachment) or pre-coated with fibronectin (10 μg/ml overnight). Specified concentrations of FGF-2 were then added and cells were harvested 10 min later for Western blots (see below for detailed procedure). Blots were first probed with anti-pErk1/2 and anti-pAkt, followed by HRP-conjugated secondary Ab and ECL detection (Amershame). Blots were then stripped and re-probed with anti-Erk1/2 and anti-Akt. Fold of stimulation is presented as pErk/Erk and pAkt/Akt ratios relative to pErk/Ekr and pAkt/Akt ratios, respectively, of control cells in SFBM. The pErk/Ekr and pAkt/Akt ratios of control cells in SFBM are used as the normalization denominator and set at an arbitrary unit of 1-fold.

Immunostaining

Cells or muscle sections were fixed for 10 min in 4% paraformaldehyde, permeabilized with 0.1% Triton-X-100 (Sigma)/PBS for 15 min at room temperature (RT), rinsed with wash buffer (0.05% Triton-X 100/PBS), treated with blocking buffer (10% Normal Goat Serum (Genetex) and 1% Blocking powder (Perkin Elmer) in wash buffer) for 1 – 2 hr, prior to incubation with primary antibodies diluted in blocking buffer overnight at 4 °C. Primary antibodies against following antigens were diluted as follows: activated β1-integrin, 1:200; β1-integrin, 1:200; BrdU, 1:200; Cleaved Caspase-3, 1:400; eMyHC, 1:200; GFP (used to detect YFP), 1:500 (rabbit) or 1:200 (chick); ILK, 1:50; Laminin, 1:2000; MHC, 1:20; MyoD, 1:50; Parvin, 1:400; Pax7, 1:20; Paxillin, 1:250; pp38, 1:50; Vinculin, 1:400. Cells or muscle sections were washed with wash buffer and incubated with appropriate Alexa-Fluor-conjugated secondary antibodies (1:1,000, Invitrogen) with various fluorescent wavelengths in blocking buffer for 1 h at RT. After wash and incubation with DAPI (1 μg/ml for 5 min), slides were then mounted with Fluoromount-G (SouthernBiotech) and coverslips (VWR). For BrdU detection, slides treated were with antigen unmasking solution (Vector) by boiling for 10 min prior to blocking and primary antibody. For EdU detection, the Click-iT reaction kit (Invitrogen) was used prior to incubation in DAPI.

Western blot

For protein extraction, cells were lysed in T-Per Tissue Protein Extraction Reagent (Thermo), 1 mM PMSF (Sigma), 1× Halt Phosphatase Inhibitor Cocktail (Thermo), and Complete Protease Inhibitor Tablet (Roche). Total protein extract was resolved by SDS-PAGE on precast gels (Bio-Rad) and then transferred to Immuno-blot PVDF Membranes (Bio-Rad) using a Bio-Rad mini-Protein II Transfer system. Membranes were rinsed in 0.1% Tween (Sigma)/TBS (20 mM Tris-HCl pH 7.5, 150 mM NaCl), blocked for 1 h at RT in 5% low-fat milk (Carnation)/0.1% Tween/TBS (blocking buffer), then incubated with primary antibodies in blocking buffer overnight at 4 °C. Primary antibodies against following antigens were used at specified dilutions: β1-integrin, 1:1000 (Millipore); Cyclin A, 1:200; Cyclin B1, 1:200; Cyclin D1, 1:200; Cyclin D2, 1:200; Cyclin D3, 1:200; Cyclin E, 1:200; Gapdh, 1:5000; pErk, Erk, pAkt, Akt, FAK, and pFAK, all at 1:1000. After washing in 0.1% Tween/TBS, appropriate secondary antibodies (Amersham, Invitrogen, and Bio-rad) were diluted 1:10,000 in blocking buffer and incubated for 1 h at RT.

Co-immunoprecipitation

HEK293T cells (Clontech, tested negative for mycoplasma contamination by MycoProbe Mycoplasma Detection Kit (R&D Systems)) were plated on fibronectin-coated 6-well dishes and transfected with pcDNA3-FGFR1-flag and/or pcDNA3-Itgb1-HA by lipofectamine2000 (Invitrogen) overnight according to manufacturer's manual. Next day, they were incubated in media containing 5 μg/ml of IgG or TS2/16 for 1 h at 4 °C. Cells were washed with cold PBS and lysed in 1% NP40 (50mM HEPES, 150mM NaCl, 10% glycerol, protease inhibitors (Thermo)) for 30 min at 4 °C. Lysates were clarified by centrifugation, and subjected to immunoprecipition by anti-HA affinity matrix (Pierce) or anti-Flag affinity matrix (Sigma) for 2 h at 4 °C. Affinity matrix were washed and proteins were eluted in 2X

SDS-PAGE sample buffer for Western blotting using anti-Flag and anti-HA antibodies (Sigma).

Force measurements and fatigue analysis

In situ force measurements of TA muscles were conducted as done previously[43,44], and the data were analyzed using the 1300A Whole Animal System (Aurora Scientific). Mice were anaesthetized with isoflurane and placed on isothermal stage. Intact TA muscles were dissected and constantly immersed in Ringer's solution. Single twitch or tetanic contractions were elicited with electrical stimulations applied by two electrodes placed on either side of the muscle. In all experiments we used 0.2 ms pulses at 10 V supramaximal voltage. Muscle optimal length (Lo) that allows a maximum isometric twitch force (Pt) was determined by a series of twitch contractions with small variations of the muscle tension. To obtain maximum isometric tetanic force (Po), muscles were stimulated for 300 ms at different frequencies from 50 to 200 Hz. A 1 min recovery period was allowed between stimulations. The muscles were then fatigued at 150 Hz with one contraction per second for 180 s. Muscle wet weight and Lo were used to calculate the cross-sectional area (CSA) of the TA muscle for normalization to obtain specific isometric twitch force sPt (kN/mm^2) and sPo (kN/mm^2).

Microscopy and image processing

Images of hematoxylin and eosin stained muscle sections were captured from a Nikon 800 microscope with 10× or 20× Plan Apo objectives and Canon EOS T3 camera using EOS Utility image acquisition software. Fluorescent images of muscle sections and single myofibers were wither captured using Leica SP5 confocal equipped with 40×/1.25 Plan Apo oil objectives using Leica image acquisition software, or a Zeiss Axioskope equipped with a 40×/0.5 Plan Apo oil objective and Axiocam camera using Zeiss image acquisition software. Identical exposure times were used and images were processed and scored with blinding using ImageJ64. If necessary, brightness and contrast were adjusted for an entire experimental image set. For quantification of polarized cell markers (Par3, m-cadherin, pp38), all authors individually scored each set of images with blinding using ImageJ64, only those that were agreed upon by all were included. For the rest, Imaris (Bitplane) was used for three-dimensional rendering of fluorescence data for quantification of polarization. A subset was also randomly selected for quantitative analysis via Imaris to confirm authors' scoring. Cell number, fiber diameter, fiber number, and fiber cross sectional area were determined using ImageJ64 or Fiji using images of a micrometer (VWR) taken under the same magnifications as the sample images as references for imaging field sizes.

FACS analysis of DNA content

For FACS analysis of DNA content, cells were collected at staggered time points post activation (24, 48, 72 h). Cells were centrifuged (2500 × g, 4 °C, 10 min) and washed twice in cold PBS. Cell pellets were resuspended in solution of 70% cold ethanol and fixed overnight at 4 °C. After washing twice with cold PBS, the cells were resuspended in 1 mL of a 1:1 PI solution (0.1 mg/mL propidium iodide in 0.6% Triton-X in PBS (Sigma; P4170)): RNase solution (2 mg/mL in milli-Q H_20 (Sigma; R5125)) and stained in the dark for 45 min. Cells were passed through meshed capped falcon tubes prior to running on FACS machine to avoid clumping. FACS analysis was carried out with a BD FACS ARIA III

machine and FACS Diva software, gating first for cell size and using forward and side scatter and then gating for YFP+ cells using the 488 channel. ModFit LT V2.2.11 was used to analyze percentages of each phase of the cell cycle, G_1, S, and G_2/M. All data were determined to have "good" RCS, measurement of fit.

RNA-seq analysis

For RNA-seq analysis, FACS isolated SCs were cultured in minimal growth media on Matrigel-coated plates. At 24, 48 and 72 h, RNA was isolated using the Arcturus PicoPure RNA isolation kit (Applied Biosystems). The Ovation RNA-Seq System (NuGEN) was used to prepare amplified cDNA. Libraries for single-end sequencing were prepared using Illumina's TruSeqDNA sample prep kit LT. Sequencing was carried out on an Illumina HiSeq2000 to generate single-end 100bp reads, which were aligned to the mouse genome (mm9) using TopHat (v2.0.7). Cufflinks (v2.1.1) was used for differential expression analysis. Only genes that displayed "yes" significance as determined by Cuffdiff 2 were analyzed further: if *P* value of observed change in FPKM was greater than the FDR (False discovery rate) after Benjamini-Hochberg correction for multiple-testing[45].

Statistical Analyses

Quantitative values are expressed as the mean ± standard deviation (s.d.) or standard error of the mean (s.e.m.). Statistical differences between groups were determined using an Excel spreadsheet by using a *t*-test for two-tailed paired comparison. When comparing more than two sets, one-way or two-way ANOVA with Tukey's *post hoc* test was performed using GraphPad Prism 6. $P < 0.05$ was determined to be significant for all experiments. All experiments requiring the use of animals or animals to derive cells were subject to randomization based on litter. No animals or samples were excluded from the study. Sample size was predetermined based on variability observed in prior experiments and preliminary data. Investigators were not blinded to outcome assessment.

Supplementary Material

Refer to Web version on PubMed Central for supplementary material.

Acknowledgments

We thank E. Dikovskaia and S. Satchell for technical assistance and C. Lepper, Y. Zheng, and lab members for comments. We especially thank A. Wagers for generously sharing the FACS and SC isolation protocol. The Carnegie Institution and National Institutes of Health (NIH) (AR060042 to C.-M.F.) provided funding for this work. M.R. is supported by a predoctoral fellowship from the NIH (HD075345), and L.L. is supported by Carnegie internal funds.

References

1. Ryall JG, Schertzer JD, Lynch GS. Cellular and molecular mechanisms underlying age-related skeletal muscle wasting and weakness. Biogerontology. 2008; 9:213–228. [PubMed: 18299960]
2. Chakkalakal JV, Jones KM, Basson MA, Brack AS. The aged niche disrupts muscle stem cell quiescence. Nature. 2012; 490:355–360. [PubMed: 23023126]
3. Fry CS, et al. Inducible depletion of satellite cells in adult, sendentary mice impairs muscle regenerative capacity without affecting sarcopenia. Nature Medicine. 2015; 21:76–80.

4. Brack AS, et al. Increased Wnt signaling during aging alters muscle stem cell fate and increases fibrosis. Science. 2007; 317:807–810. [PubMed: 17690295]
5. Cosgrove BD, et al. Rejuvenation of the muscle stem cell population restores strength to injured aged muscles. Nature Medicine. 2014; 20:255–264.
6. Conboy IM, Conboy MJ, Smythe GM, Rando TA. Notch-mediated restoration of regenerative potential to aged muscle. Science. 2003; 302:1575–1577. [PubMed: 14645852]
7. Shea KL, et al. Sprouty1 regulates reversible quiescence of a self-renewing adult muscle stem cell pool during regeneration. Cell Stem Cell. 2010; 6:117–129. [PubMed: 20144785]
8. Carlson ME, Hsu M, Conboy IM. Imbalance between pSmad3 and Notch induces CDK inhibitors in old muscle stem cells. Nature. 2008; 454:528–532. [PubMed: 18552838]
9. Bernet JD, et al. p38 MAPK signaling underlies a cell-autonomous loss of stem cell self-renewal in skeletal muscle of aged mice. Nature Medicine. 2014; 20:265–271.
10. Price FD, et al. Inhibition of JAK-STAT signaling stimulates adult satellite cell function. Nature Medicine. 2014; 20:1174–1181.
11. Tierney MT, et al. STAT3 signaling controls satellite cell expansion and skeletal muscle repair. Nature Medicine. 2014; 20:1182–1186.
12. Mori S, Takada Y. Crosstalk between Fibroblast Growth Factor (FGF) Receptor and Integrin through Direct Integrin Binding to FGF and Resulting Integrin-FGF-FGFR Ternary Complex Formation. Medical Sciences. 2013; 1:20–36.
13. Assoian RK, Schwartz MA. Coordinate signaling by integrins and receptor tyrosine kinases in the regulation of G1 phase cell-cycle progression. Curr Opin Genet Dev. 2001; 11:48–53. [PubMed: 11163150]
14. Hynes RO. Integrins: bidirectional, allosteric signaling machines. Cell. 2002; 110:673–687. [PubMed: 12297042]
15. Helbling-Leclerc A, et al. Mutations in the laminin alpha 2-chain gene (LAMA2) cause merosin-deficient congenital muscular dystrophy. Nature Genetics. 1995; 11:216–218. [PubMed: 7550355]
16. Schwander M, et al. Beta1 integrins regulate myoblast fusion and sarcomere assembly. Developmental Cell. 2003; 4:673–685. [PubMed: 12737803]
17. Bulfield G, Siller WG, Wight PA, Moore KJ. X chromosome-linked muscular dystrophy (mdx) in the mouse. Proceedings of the National Academy of Sciences of the United States of America. 1984; 81:1189–1192. [PubMed: 6583703]
18. Lepper C, Conway SJ, Fan CM. Adult satellite cells and embryonic muscle progenitors have distinct genetic requirements. Nature. 2009; 460:627–631. [PubMed: 19554048]
19. Raghavan S, Bauer C, Mundschau G, Li Q, Fuchs E. Conditional ablation of beta1 integrin in skin. Severe defects in epidermal proliferation, basement membrane formation, and hair follicle invagination. J Biophys Biochem Cytol. 2000; 150:1149–1160.
20. Webster MT, Fan CM. c-MET regulates myoblast motility and myocyte fusion during adult skeletal muscle regeneration. PLoS ONE. 2013; 8:e81757. [PubMed: 24260586]
21. Roovers K, Davey G, Zhu X, Bottazzi ME, Assoian RK. Alpha5beta1 integrin controls cyclin D1 expression by sustaining mitogen-activated protein kinase activity in growth factor-treated cells. Mol Biol Cell. 1999; 10:3197–3204. [PubMed: 10512860]
22. Polanska UM, Fernig DG, Kinnunen T. Extracellular interactome of the FGF receptor–ligand system: Complexities and the relative simplicity of the worm. Developmental Dynamics. 2009; 238:277–293. [PubMed: 18985724]
23. Murakami M, Elfenbein A, Simons M. Non-canonical fibroblast growth factor signalling in angiogenesis. Cardiovascular Research. 2008; 78:223–231. [PubMed: 18056763]
24. Miyamoto S, Teramoto H, Gutkind JS, Yamada KM. Integrins can collaborate with growth factors for phosphorylation of receptor tyrosine kinases and MAP kinase activation: roles of integrin aggregation and occupancy of receptors. J Biophys Biochem Cytol. 1996; 135:1633–1642.
25. Jones NC, Fedorov YV, Rosenthal RS, Olwin BB. ERK1/2 is required for myoblast proliferation but is dispensable for muscle gene expression and cell fusion. J Cell Physiol. 2001; 186:104–115. [PubMed: 11147804]

26. Siegel AL, Atchison K, Fisher KE, Davis GE, Cornelison D. 3D Timelapse Analysis of Muscle Satellite Cell Motility. Stem Cells. 2009; 27:2527–2538. [PubMed: 19609936]
27. Troy A, et al. Coordination of satellite cell activation and self-renewal by Par-complex-dependent asymmetric activation of p38α/β MAPK. Cell Stem Cell. 2012; 11:541–553. [PubMed: 23040480]
28. Conboy IM, et al. Rejuvenation of aged progenitor cells by exposure to a young systemic environment. Nature. 2005; 433:760–764. [PubMed: 15716955]
29. Kragstrup TW, Kjaer M, Mackey AL. Structural, biochemical, cellular, and functional changes in skeletal muscle extracellular matrix with aging. Scandinavian Journal of Medicine & Science in Sports. 2011; 21:749–757. [PubMed: 22092924]
30. Wood LK, et al. Intrinsic stiffness of extracellular matrix increases with age in skeletal muscles of mice. J Appl Physiol. 2014; 117:363–369. [PubMed: 24994884]
31. Bazzoni G, Shih DT, Buck CA, Hemler ME. Monoclonal Antibody 9EG7 Defines a Novel β1 Integrin Epitope Induced by Soluble Ligand and Manganese, but Inhibited by Calcium. J Biol Chem. 1995; 270:25570–25577. [PubMed: 7592728]
32. Takagi J, Springer TA. Integrin activation and structural rearrangement. Immunological Reviews. 2002; 186:141–163. [PubMed: 12234369]
33. Calderwood DA, Shattil SJ, Ginsberg MH. Integrins and actin filaments: reciprocal regulation of cell adhesion and signaling. J Biol Chem. 2000; 275:22607–22610. [PubMed: 10801899]
34. Hintermann E, Bilban M, Sharabi A, Quaranta V. Inhibitory role of alpha 6 beta 4-associated erbB-2 and phosphoinositide 3-kinase in keratinocyte haptotactic migration dependent on alpha 3 beta 1 integrin. J Biophys Biochem Cytol. 2001; 153:465–478.
35. Toledo MS, Suzuki E, Handa K, Hakomori S. Effect of ganglioside and tetraspanins in microdomains on interaction of integrins with fibroblast growth factor receptor. J Biol Chem. 2005; 280:16227–16234. [PubMed: 15710618]
36. Sahni A, Francis CW. Stimulation of endothelial cell proliferation by FGF-2 in the presence of fibrinogen requires alphavbeta3. Blood. 2004; 104:3635–3641. [PubMed: 15297314]
37. Sicari BM, et al. An acellular biologic scaffold promotes skeletal muscle formation in mice and humans with volumetric muscle loss. Sci Transl Med. 2014; 6:234ra58.
38. Fukada SI, et al. Molecular signature of quiescent satellite cells in adult skeletal muscle. Stem Cells. 2007; 25:2448–2459. [PubMed: 17600112]
39. Tanentzapf G, Devenport D, Godt D, Brown NH. Integrin-dependent anchoring of a stem-cell niche. Nat Cell Biol. 2007; 9:1413–1418. [PubMed: 17982446]
40. Soriano P. Generalized lacZ expression with the ROSA26 Cre reporter strain. Nature Genetics. 1999; 21:70–71. [PubMed: 9916792]
41. Srinivas S, et al. Cre reporter strains produced by targeted insertion of EYFP and ECFP into the ROSA26 locus. BMC Dev Biol. 2001; 1:4. [PubMed: 11299042]
42. Hogan, B.; Beddington, R.; Cstantini, F.; Lacey, E. Manipulating the mouse embryo. Cold Spring Harbor Laboratory Press; 1994.
43. Hakim CH, Wasala NB, Duan D. Evaluation of Muscle Function of the Extensor Digitorum Longus Muscle Ex vivo and Tibialis Anterior Muscle In situ in Mice. J Vis Exp. 2013; 21
44. Barton ER, Khurana TS, Lynch GS. Measuring isometric force of isolated mouse muscles in vitro. TREAT-NMD. 2008
45. Trapnell C, et al. Differential analysis of gene regulation at transcript resolution with RNA-seq. Nature Biotech. 2012; 31:46–53.

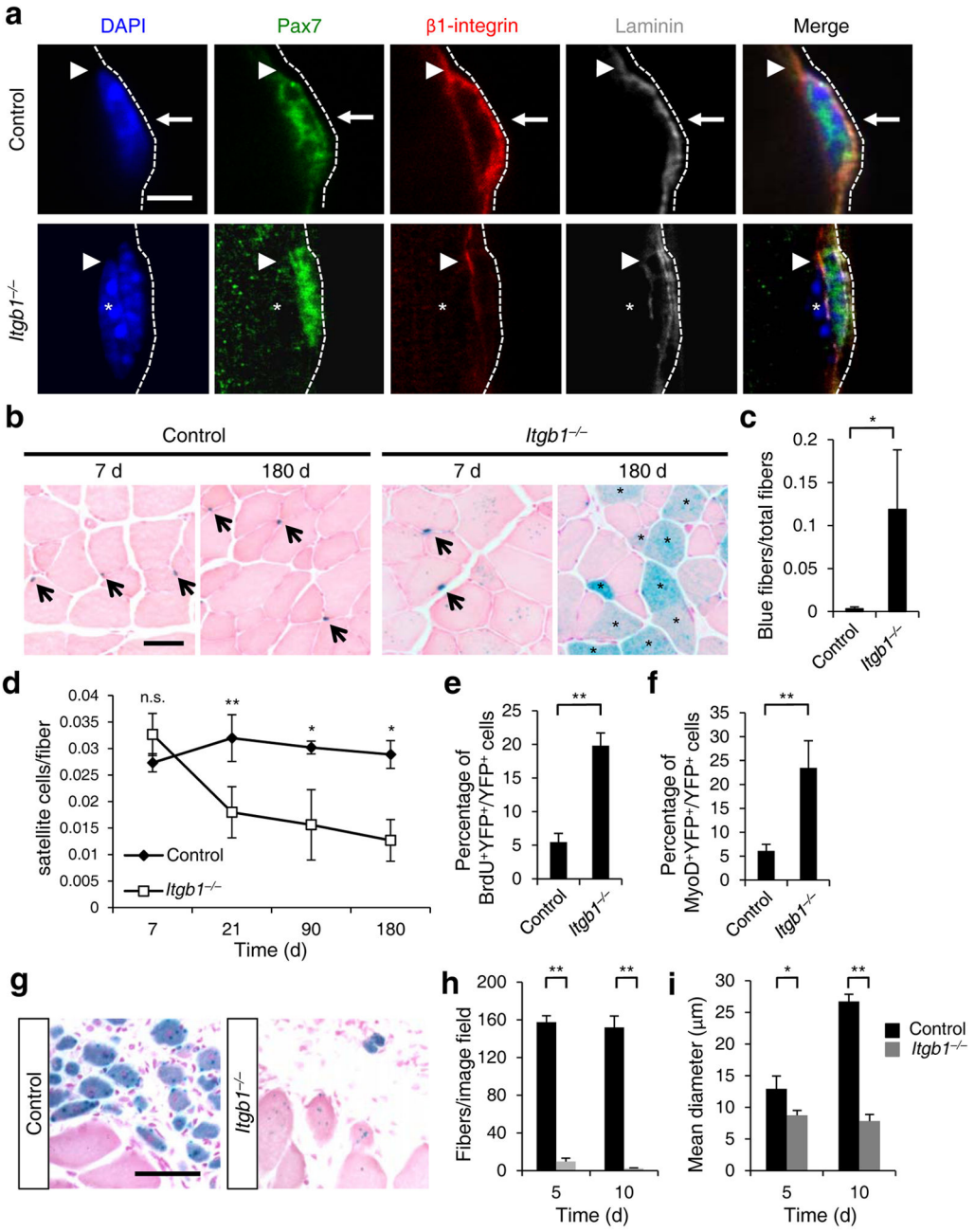

Figure 1.

Young *Itgb1*$^{-/-}$ SCs are defective in maintaining quiescence and sustaining regeneration. (**a**) Control and *Itgb1*$^{-/-}$ SCs on myofibers (assay scheme in Supplementary Fig. 1a) stained for Pax7, β1-integrin, and laminin (dotted line); arrows, basal β1-integrin in SC; arrowheads, muscle β1-integrin; asterisks, myonucleus; Scale bar, 5 μm. (**b**–**d**) Long-term tracing of β-gal lineage-marked (*R26R*^{LacZ} reporter) control and mutant SCs after tmx regimen: (**b**) X-gal reacted (blue) and nuclear fast red stained muscle sections at 7 and 180 d; arrows, SCs; asterisks, X-gal^{+} myofibers. (**c**) Quantified blue fibers per field using data in (**b**). (**d**) SC to fiber ratios at 7, 21, 90, and 180 d; $n = 3$ animals per group, ten sections scored per animal.

(**e**) Percentages of $BrdU^+YFP^+$/total YFP^+ cells of control and *Itgb1*$^{-/-}$ muscles after 1 month of BrdU administration; $n = 3$ animals per group, ten sections scored per animal. (**f**) Percentages of $MyoD^+YFP^+/YFP^+$ cells from the same animals in **e**. (**g**) Representative images ($n > 15$ per condition) of X-gal reacted control and *Itgb1*$^{-/-}$ muscle sections at 5 d post CTX injury (scheme in Supplementary Fig. 3a); Scale bar, 25 μm. (**h**,**i**) Average fiber number per field (0.228 μm^2) (**h**) and mean fiber diameter (**i**) at 5 d and 10 d post injury; $n =$ 3 animals per group, 20 sections scored per animal. All numerical data are presented as mean ± s.d.; Student's *t*-test: $*P < 0.05$, $**P < 0.01$, and n.s., not significant.

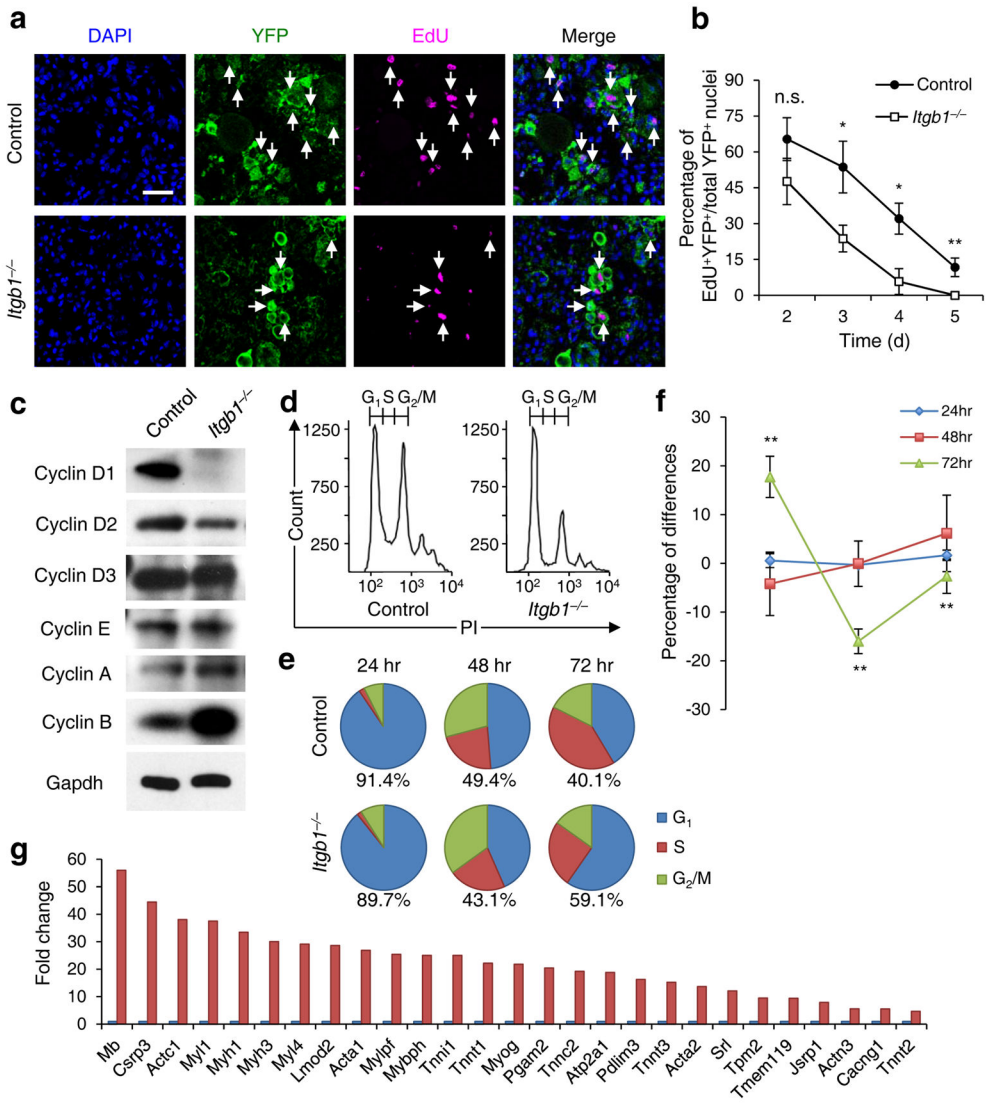

Figure 2.

Young *Itgb1*$^{-/-}$ SCs are defective in maintaining proliferation and prone to differentiation. (**a**) EdU incorporation of YFP^{+} control and mutant cells in muscle sections 3 d after injury; Scale bar, 50 μm. (**b**) Quantification of EdU^{+}YFP^{+}/YFP^{+} on d 2 – 5 daily; data are expressed as mean ± s.d., $n = 3$ animals per d; ten sections per sample; Student's t-test: $^{*}P < 0.05$, $^{**}P < 0.01$, and n.s., non-significant. (**c**) Western blot of FACS isolated control and *Itgb1*$^{-/-}$ YFP^{+} SCs cultured for 72 h, using antibodies to proteins indicated. (**d**–**f**) FACS-aided cell cycle analyses using DNA content (stained by PI) of control and mutant SCs at 24, 48, and 72 h: (**d**) PI profiles at 72 h, (**e**) pie charts summarize cell fractions in G1, S, and G2/M, and (**f**) percentage deviation plot of mutant vs. control cells in cell cycle phases at stipulated time points; ModFit LT V2.2.11 was used to analyze percentages of each phase of the cell cycle. All data were determined to have "good" RCS, measurement of fit. (**g**) Fold changes of muscle differentiation genes upregulated in *Itgb1*$^{-/-}$ SCs compared to control SCs at 72 h. All listed genes display "yes" significance (q < 0.05) by Cuffdiff2, Genes were

included only if one (control or *Itgb1*$^{-/-}$) had FPKM ≥5 to control for elevated fold changes of genes with minimal expression.

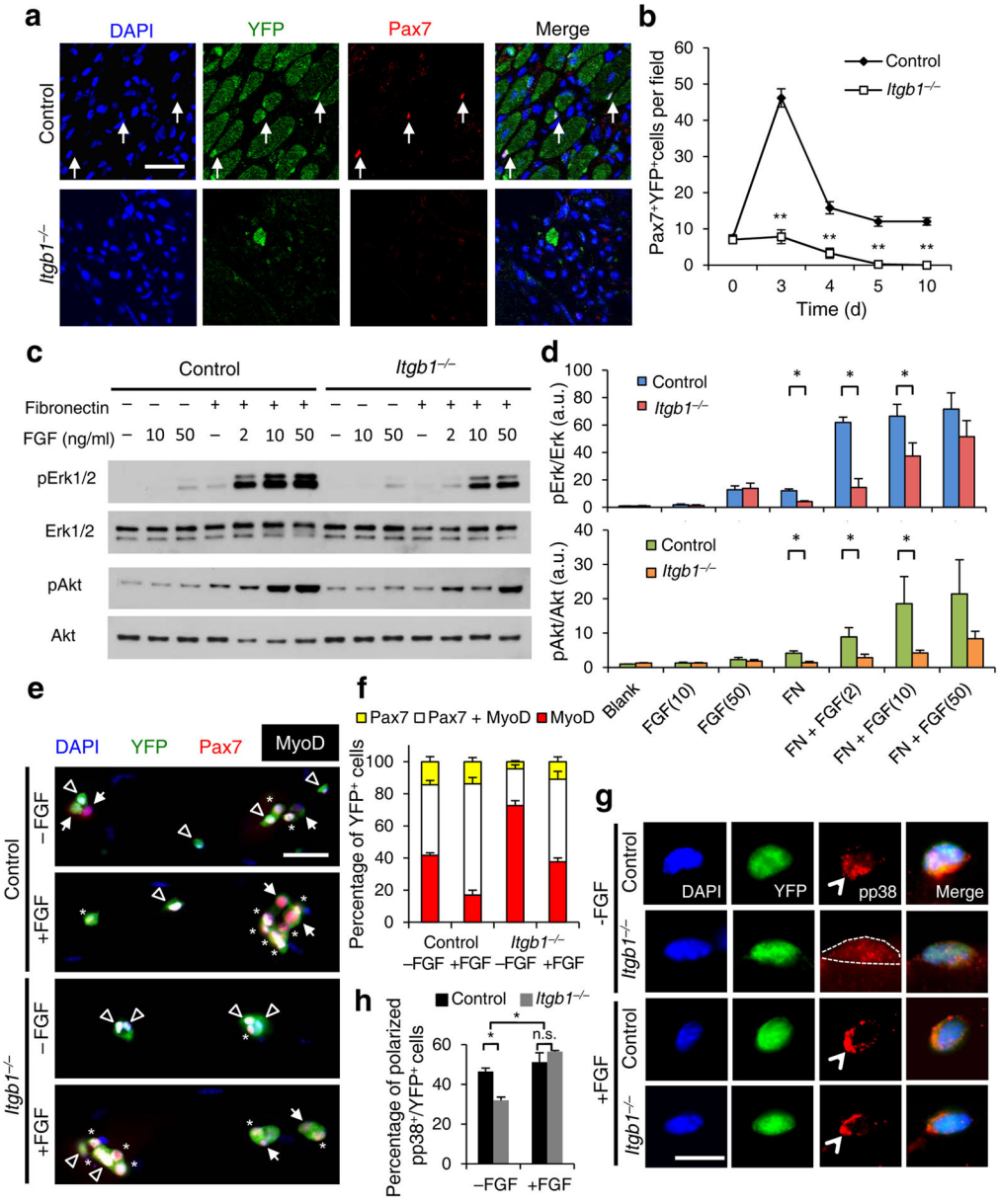

Figure 3.

Itgb1$^{-/-}$ SCs show a compromised response to FGF-2 that can be partially restored by exogenous FGF-2. (**a**) Control and *Itgb1*$^{-/-}$ sections 10 d after injury stained for Pax7 and YFP; arrows, Pax7^{+} SCs; Scale bar, 25 μm. (**b**) Average number of Pax7^{+}YFP^{+} cells per field (0.228 μm^{2}) during regeneration; $n = 3$ animals per time point, ten sections per animal; data are expressed as mean ± s.d.; Student's *t*-test: $*P < 0.05$; $**P < 0.01$. (**c**) Western blots for pErk1 and pErk2, Erk1 and Erk2, pAkt, and Akt of control and *Itgb1*$^{-/-}$ cells. Fibronectin addition (+) and FGF-2 concentrations (FGF(ng/ml)) are indicated. (**d**) Fold induction from data in **c**, normalized to control cells without fibronectin and FGF-2 (set at 1 arbitrary unit (a.u.)); $n = 4$ parallel sets of myoblasts. Paired comparisons with significant differences are indicated; data are expressed as mean ± s.e.m.; two-way ANOVA: $*P < 0.05$.

(**e**) Control and *Itgb1*$^{-/-}$ SCs cultured for 96 h with or without 10 ng/ml FGF-2 were stained for YFP, Pax7, MyoD, and DAPI; arrows, Pax7^{+} cells, asterisks, Pax7^{+}MyoD^{+} cells, and triangles, MyoD^{+} cells; scale bar = 25 μm. (**f**) Percentage distribution of various cell populations from data in (**e**); $n = 3$ animals; ≥ 20 myofibers per condition; two-way ANOVA: $P < 0.01$ for Pax7^{+}MyoD^{+} and MyoD^{+}, −FGF vs. +FGF (control and *Itgb1*$^{-/-}$), control vs. *Itgb1*$^{-/-}$ (−FGF and +FGF); $P < 0.05$ for Pax7^{+}, control vs. *Itgb1*$^{-/-}$ (−FGF). (**g**) Representative images ($n = 25$) of YFP^{+} SCs cultured for 36 h with or without FGF-2 were stained for pp38; polarized, open arrowheads; non-polarized, dashed outline; Scale bar, 10 μm. (**h**) Percentages of YFP^{+} SCs with polarized pp38^{+} from data in **g**; numerical data are expressed as mean ± s.d.; $n = 3$ experiments, ≥ 25 myofibers per condition. Data were compared by two-way ANOVA: $*P < 0.05$ and n.s., not significant.

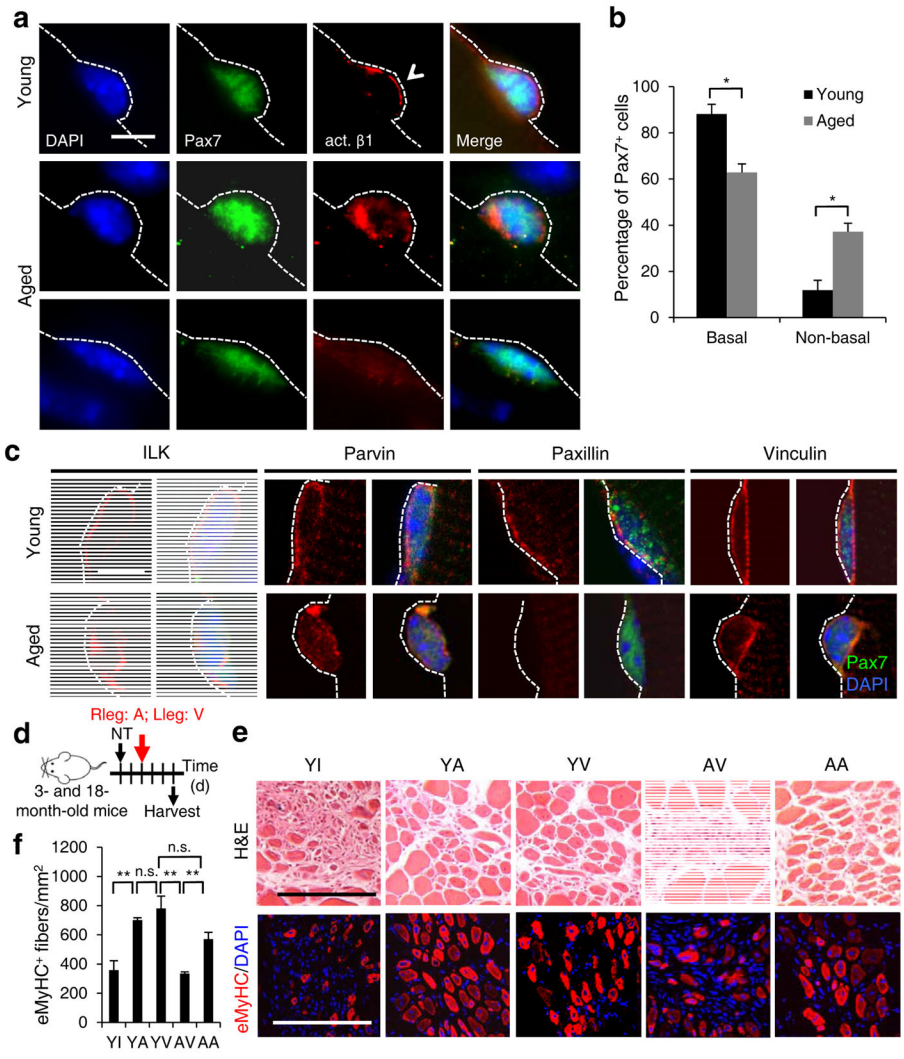

Figure 4.

Activating β1-integrin in aged SCs can rescue aged-associated SC defects. (**a**,**b**) Myofiber-associated young and aged SCs stained for Pax7, activated β1-integrin (act. β1), and DAPI 1 h after isolation; basal surface, dashed line; act. β1 patterns scored as basal (open arrowhead) or unevenly or non-detectable (non-basal) in **b**; Scale bar, 10 μm. All images were taken with same exposure. (**b**) Percentages of Pax7$^+$ SCs scored by act. β1 patterns from **a**; $n = 3$ experiments, ≥ 20 myofibers; numerical data are expressed as mean ± s.d.; Student's t-test: $^*P < 0.05$. (**c**) Young and aged Pax7$^+$ SCs stained for ILK, Parvin, Paxillin, Vinculin, and DAPI 1 h after isolation; dashed lines, basal surface; scale bar = 5 μm. All images were taken with same exposure. (**d**) Schematic for β1-integrin activation in young (3 month) or aged (18 month) muscles after needle track injury. 2 d post injury, IgG vehicle (10 μg/ml; V), TS2/16 activating antibody (10 μg/ml; A), or RGD peptide inhibitor (10 μg/m; I) were injected into the injury site. Muscles were harvested 3 d later. (**e**) Muscle sections were stained for H&E or eMyHC; Scale bar, 150 μm. (**f**) Average number of eMyHC$^+$ fibers in injured areas of each group; data represent mean ± s.d.; $n = 3$; ten sections per animal; two-way ANOVA: $^{**}P < 0.01$ and n.s., not significant.

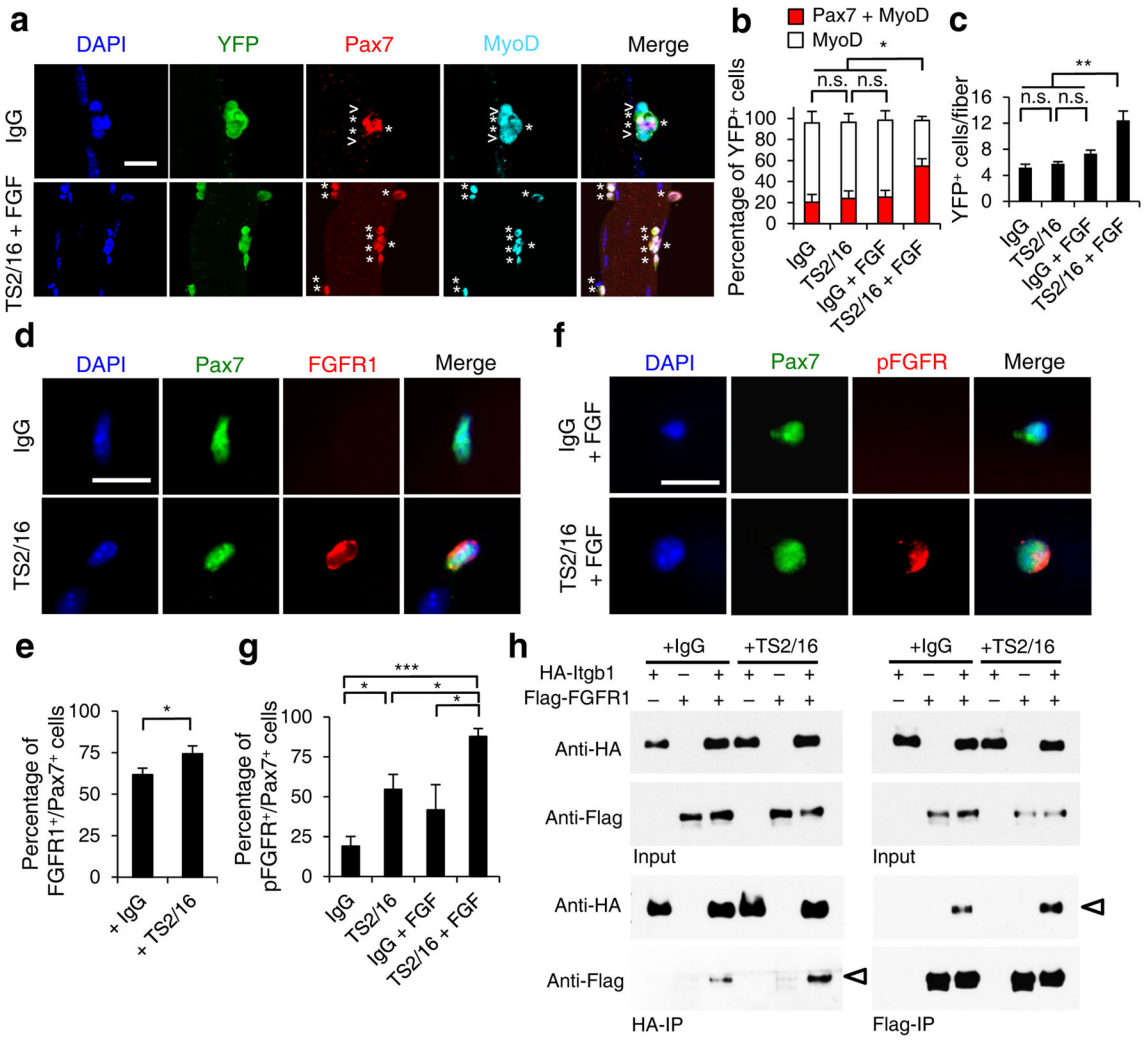

Figure 5.

Activating β1-integrin in aged SCs enhances FGF signaling to promote SC expansion. (**a**–**c**) Myofiber-associated YFP$^+$ aged SCs were cultured with IgG or TS2/16 (at 10 μg/ml) and with or without FGF-2 (FGF, 10 ng/ml) for 72 h, and stained for Pax7 and MyoD. (**a**) Images for IgG alone and TS2/16 + FGF-2 treated cultures; asterisk, Pax7$^+$MyoD$^+$ cells; open arrowhead, MyoD$^+$ cells; Scale bar, 25 μm. (**b**) Percentages of Pax7$^+$MyoD$^+$ versus MyoD$^+$ cells in all four groups; mean ± s.d.; $n = 3$ experiments, ≥ 30 myofibers each; two-way ANOVA: $*P < 0.05$ for TS2/16 + FGF-2 versus others, and not significant (n.s.) between the other groups. (**c**) Average number of YFP$^+$ cells per myofiber of the same samples in **a**; mean ± s.d.; n = 3 animals, ≥ 15 myofibers each two-way ANOVA: $**P < 0.01$ for TS2/16 + FGF-2 versus others, and n.s. between the other groups. (**d**,**e**) Myofiber-associated aged SCs cultured for 24 h with IgG or TS2/16 and stained for Pax7 and FGFR1. (**d**) Representative images ($n = 20$); Scale bar, 10 μm. (**e**) Percentage of FGFR1$^+$ cells within the Pax7$^+$ population; mean ± s.d., $n = 3$ experiments, ≥ 20 myofibers per condition; Student's t-test: $*P < 0.05$. (**f**,**g**) Aged SCs cultured with IgG or TS2/16, and with or without FGF-2, were stained for phospho-FGFR (pFGFR) and Pax7. (**f**) Representative images of

IgG + FGF-2 and TS2/16 + FGF-2 (n = 20 images of each group); Scale bar, 10 μm. (**g**) Percentage of $pFGFR^+$ cells within the $Pax7^+$ SC population; mean ± s.d.; n = 3 experiments, ≥ 20 myofibers scored per condition; Student's t-test: $*P < 0.05$, $***P < 0.001$. (**h**) Reciprocal co-immunoprecipitation (co-IP) between HA-tagged Itgb1 and Flag-tagged FGFR1 in HEK293T cells, with IgG or TS2/16 added, followed by Western blot; input lysates, top two rows; IPed fractions, bottom two rows; antibodies for IP, labeled at bottom, and for Western blots, left. Open arrowheads indicate co-IPed Flag-FGFR1 (left) and HA-Itgb1 (right).

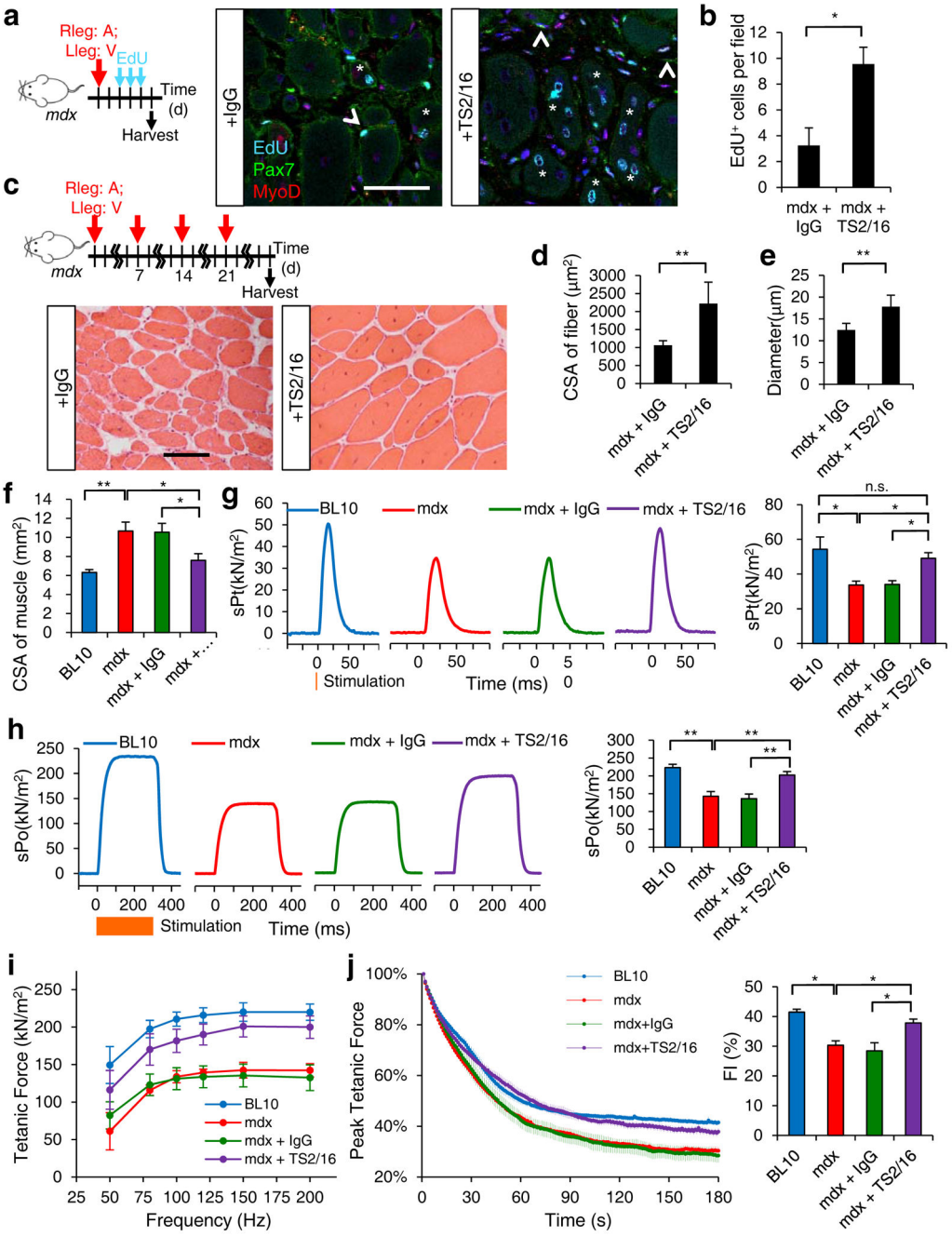

Fig. 6.

Activating β1-integrin in *mdx* mice ameliorates dystrophic pathology and restores muscle strength. (**a**) Schematic of short-term IgG (V) and TS2/16 (A) treatment of 3 month old *mdx* mice and images of EdU$^+$ myogenic nuclei that are Pax7$^+$, MyoD$^+$ (open arrowheads), or centrally located (asterisk). (**b**) Number of EdU$^+$ nuclei per field (0.228μm^2); $n = 3$ animals per treatment; ten sections per animal. (**c**) Schematic of long-term IgG or TS2/16 treatment and images of H&E stained muscle sections of treated *mdx* mice at 28 d; Scale bar, 25 μm. (**d**) Cross-sectional area (CSA) and (**e**) diameter of myofbers from data in **c**; $n = 3$ animals

per treatment, ten sections per animal; mean ± s.d.; Student's *t*-test: $*P < 0.05$, $**P < 0.01$. (**f**) CSA of TA muscles from 4 groups of 3 month old mice: C57BL/10 (BL10, untreated), *mdx* (untreated), *mdx* + IgG (IgG treated), *mdx* + TS2/16 (TS2/16-treated); the latter two groups were treated by regimen in **d**. (**g**–**j**) Contractile properties of TA muscles were measured *in situ*: (**g**) Representative traces ($n = 5$ per group)of normalized specific twitch force (sPt) and quantifications; orange vertical line, time of stimulation. (**h**) Representative traces ($n = 5$ per group)for specific maximum tetanic forces (sPo) and quantifications; orange bar, duration of stimulation (300 ms). (**i**) Normalized tetanic force to stimulation frequency relationship. (**j**) Fatigue traces (left) over 180 s and fatigue indices (FI = tetanic $force_{t0}$/tetanic $force_{t180}$) for all groups. Numerical data are expressed as mean ± s.d.; Student's *t*-test: $*P < 0.05$, $**P < 0.01$, and n.s., not significant.